



Published in final edited form as:

Arterioscler Thromb Vasc Biol. 2008 November ; 28(11): 1982–1988. doi:10.1161/ATVBAHA.108.169722.

Vascular Inflammation, Insulin Resistance and Reduced Nitric Oxide Production Precede the Onset of Peripheral Insulin Resistance

Francis Kim^{1,2}, Matilda Pham¹, Ezekiel Maloney¹, Norma O. Rizzo¹, Gregory J. Morton^{1,2}, Brent E. Wisse^{1,2}, Elizabeth A. Kirk³, Alan Chait^{1,2}, and Michael W. Schwartz^{1,2}

¹ Department of Medicine University of Washington, Seattle, WA 98104

² Diabetes and Obesity Center of Excellence, University of Washington, Seattle, WA 98104

³ Department of Epidemiology and Nutritional Sciences Program University of Washington, Seattle, WA 98104

Abstract

Objectives—Obesity causes inflammation and insulin resistance in the vasculature as well as in tissues involved in glucose metabolism such as liver, muscle, and adipose tissue. To investigate the relative susceptibility of vascular tissue to these effects, we determined the time course over which inflammation and insulin resistance develops in various tissues of mice with diet-induced obesity (DIO) and compared these tissue-based responses to changes in circulating inflammatory markers.

Methods and results—Adult male C57BL/6 mice were fed either a control low-fat diet (LF; 10% saturated fat) or a high-fat diet (HF, 60% saturated fat) for durations ranging between 1-14 wk. Cellular inflammation and insulin resistance were assessed by measuring phospho-I κ B α and insulin-induced phosphorylation of Akt, respectively, in extracts of thoracic aorta, liver, skeletal muscle and visceral fat. As expected, HF feeding induced rapid increases of body weight, fat mass, and fasting insulin levels compared to controls, each of which achieved statistical significance within 4 weeks. Whereas plasma markers of inflammation became elevated relatively late in the course of DIO (e.g., serum amyloid A (SAA), by Week 14), levels of phospho-I κ B α in aortic lysates were elevated by 2-fold within the first week. The early onset of vascular inflammation was accompanied by biochemical evidence of both endothelial dysfunction (reduced nitric oxide production; induction of intracellular adhesion molecule-1 (ICAM-1) and vascular cell adhesion molecule-1 (VCAM-1)) and insulin resistance (impaired insulin-induced phosphorylation of Akt and eNOS). Although inflammation and insulin resistance were also detected in skeletal muscle and liver of HF-fed animals, these responses were observed much later (between 4 and 8 wk of HF feeding), and they were not detected in visceral adipose tissue until 14 wk.

Conclusions—During obesity induced by HF feeding, inflammation and insulin resistance develop in the vasculature well before these responses are detected in muscle, liver or adipose tissue. This observation suggests that the vasculature is more susceptible than other tissues to the deleterious effects of nutrient overload.

Keywords

Nitric Oxide; vascular inflammation; eNOS; insulin resistance; obesity

Introduction

The effect of obesity to increase risk of cardiovascular morbidity and mortality is strongly associated with insulin resistance in peripheral tissues such as liver, skeletal muscle, and adipose tissue. Growing evidence suggests that in animal models of both genetic (e.g., the Fatty Zucker rat) and acquired (e.g., diet-induced obesity or DIO) obesity, the pathogenesis of insulin resistance in these key metabolic tissues involves activation of IKK β and subsequently of NF- κ B, a key transcriptional mediator of cellular inflammation.^{1,2} Similarly, impaired insulin signaling in cultured endothelial cells occurs rapidly following exposure to free fatty acids (FFA) or excess glucose via a mechanism that is dependent on activation of IKK β ,^{3, 4} and both cellular inflammation and insulin resistance are also observed in vascular tissue taken from obese Zucker rats (fa/fa)⁵ or mice with DIO.⁶ These observations suggest that at the cellular level, the vasculature is affected by nutrient overload via mechanisms closely related to those that cause insulin resistance in key tissues involved in glucose homeostasis. Interestingly, the deleterious effect of nutrient excess on endothelial cells appears within the first few hours of exposure,⁴ whereas response of other cell types to nutrient excess often takes longer to develop.⁷ These observations prompted us to ask whether the susceptibility of vascular tissue to inflammation and insulin resistance is greater than in other tissue types, and thus occurs earlier in the course of DIO.

Although the key, early role of reduced nitric oxide (NO) production in the development of vascular disease such as hypertension and atherosclerosis is well described, the temporal relationship between the onset of reduced NO bioavailability and that of peripheral insulin resistance remains an important unanswered question. Clinical studies have demonstrated that a consumption of a single high-fat meal acutely decreases brachial reactivity,⁸ a non-invasive measure of NO production, and that consuming a diet high in saturated fats for 3 weeks also causes significant endothelial dysfunction.⁹ These observations suggest that even brief exposure to nutrient excess reduces NO bioavailability and that this effect may develop well before the onset of obesity, systemic inflammation, and insulin resistance. In addition to measures of inflammation and insulin resistance, therefore, we also determined the time course over which DIO leads to reduced endothelial nitric oxide (NO) production, establishing its temporal association with onset of vascular inflammation and insulin resistance.

To accomplish these goals, the present study employed a mouse model of DIO induced by high-fat feeding to assess the natural history of inflammation and impaired insulin signaling in four different insulin-sensitive tissues: vascular tissue (thoracic aorta), liver, adipose tissue and skeletal muscle. Our finding that vascular tissue is adversely impacted much earlier in the course of DIO than are key insulin-sensitive tissues involved in glucose metabolism implies a heightened susceptibility of vascular elements to the deleterious effects of obesity.

Methods

Materials

Anti-phospho-eNOS (Ser1177), phospho-Akt (Ser473), anti-Akt, anti-phospho-I κ B α antibodies were obtained from Cell Signaling (Beverly, MA), anti-eNOS antibody was obtained from Transduction Labs, BD Biosciences (Lexington, Kentucky) and anti-ICAM antibody (R and D Systems, Minneapolis, MN). Total Akt and pAkt(serine 473) ELISA kits were obtained from Biosource (Camarillo, CA). Sodium DETC was obtained from Alexis Biochemical (Lausen, Switzerland). FeSO₄ 7H₂O was purchased from Sigma (St Louis, MO) Fluorokine MAP Multiplex base kit and analyte kits (IL-6, CCL2/JE (MCP-1), IL- β), (R and D Systems, Minneapolis, MN). Vascular cell adhesion molecule-1 (VCAM-1) and TNF- α gene expression levels were measured using TaqMan Gene expression Assays (Applied Biosystems).

Study protocol

Adult male C57BL/6 mice were purchased from Jackson Laboratories and were maintained in a temperature-controlled facility with a 12-hour light-dark cycle. Age-matched groups (6-12 wk of age; n=10 per group) were fed an equicaloric diet that was either low (10% saturated fat) or high in fat content (60% saturated fat) (Research Diets, numbers D12492, D12450B) for periods ranging from 1-14 weeks. Body weight and food intake were measured weekly and body composition was measured in unanesthetized animals serially at baseline, 4 wk, and 8 wk by MRS (Echo Medical Systems) in the University of Washington Clinical Nutrition Research Unit Animal Studies Core Laboratory.¹⁰

At the conclusion of the study, one-half of the animals in each study group received an IP injection of either vehicle (normal saline) or regular insulin (0.06 U/g body weight in 300 μ l of normal saline) after an overnight fast. Fifteen minutes later, mice were euthanized with an overdose of CO₂ followed by cervical dislocation. Thoracic aorta, liver, skeletal muscle (quadriceps), and adipose tissue (mesenteric) were removed and snap frozen on dry ice after dissecting away surrounding connective tissue. Protein was subsequently extracted from tissue samples and, after protein levels were quantified (Micro BCA Protein Assay Kit; Pierce, Rockford II), equal amounts of protein were used for each condition in each assay. Total Akt and phospho-Akt (serine 473) levels were determined using ELISA assay kits (Biosource). Total eNOS, peNOS, phospho-I κ B α , and ICAM levels were assessed using Western blot analysis using gradient 4 \times 20% Tris-Glycine gels (Lonza; Rockland, Me) and Fermentas PageRuler Prestained Protein Ladder was used to determine the protein band of interest which was then quantified using Image J software (NIH). All study protocols were approved by the University of Washington Institutional Animal Care and Use Committee.

Nitric Oxide measurement

Nitric oxide was measured using the spin trap Fe(DETC)₂ which was first reported and validated by Kleschyov et al.¹¹ Preparation of colloid Fe(DETC)₂: Sodium DETC (3.6 mg) and FeSO₄ 7H₂O (2.25 mg) were dissolved under argon gas in 10 ml of ice cold Krebs-Hepes buffer¹² (consisting of, in mM: NaCl 99, KCl 4.7, MgSO₄ 1.2, KH₂PO₄ 1.0, CaCl₂ 1.9, NaHCO₃ 25, glucose 11.1, and Na-Hepes 20, pH7.4) These were rapidly mixed to obtain a pale yellow-brown colored Fe(DETC)₂ solution which was used immediately. Thoracic aortas were cleaned of adhering fat and soft tissue and kept in ice-cold Krebs solution, aortic samples were sectioned and separated into 6 well plates each containing 100 μ l of Krebs-hepes buffer. Colloid Fe(DETC)₂ was then added to final concentration of 286 μ M and incubated at 37 °C for 90 minutes.

Electron spin resonance spectroscopy (ESR) studies were performed on a table-top x-band spectrometer Miniscope (Magnettech, Germany). Recordings were made at 77 K using a Dewar flask. Instrument settings were 10 mW of microwave power, 1 mT of amplitude modulation, 100 kHz of modulation frequency, 20 s of sweep time and 10 number of scans.

Plasma cholesterol, insulin, and cytokine measurements

Blood samples were placed on ice until separation of plasma by centrifugation. Total plasma cholesterol and triglyceride levels were determined in the fasted condition using the DCL Total Cholesterol Assay Kit and Roche Diagnostics Triglyceride Assay. Insulin levels were determined using an ELISA kit (Crystal Chem Inc, Downers Grove, IL), and glucose levels were determined by glucometer (FreeStyle, TheraSense, Alameda, CA). Serum cytokines were measured using a bead-based cytometric immunoassay system (Luminex). Serum SAA levels were measured as previously described.¹³

Statistical analysis

In all experiments, densitometry measurements were normalized to controls incubated with vehicle and percent change relative to the control condition was calculated. Analysis of the results was performed using the STATA8 statistical package. Data are expressed as mean \pm SEM, and values of $p < 0.05$ were considered statistically significant. A two-tailed *t*-test was used to compare mean values from studies involving two experimental groups. To compare responses following treatment with vehicle or insulin across the two diets, data were analyzed by two-way analysis of variance using the Bonferoni-post-hoc comparison test.

Results

Effect of high-fat feeding on body weight, fat content, metabolic parameters, and systemic markers of inflammation

As expected, body weight increased steadily over the 14-week study period among mice fed a HF diet compared to LF-fed controls, and this effect became statistically significant after 4 weeks of high-fat feeding (Supplemental Figure IA). Similarly, differences between LF and HF groups with respect to both percent body fat (Supplemental Figure IB) and total fat mass (baseline: 2.8 ± 0.3 g vs. 2.5 ± 0.5 g ($p = \text{NS}$); 4 weeks: 3.2 ± 1.2 g vs. 9.2 ± 2.5 g ($p < 0.05$); 8 weeks: 6.5 ± 2.5 g vs. 12.1 ± 1.9 g ($p < 0.05$)) became significant by 4 wk.

Whereas fasting insulin levels remained relatively constant over the 14 wk study in LF-fed mice, fasting insulin levels in HF-fed mice were increased by almost 4-fold by the 4 wk time point, consistent with the development of insulin resistance, and remained significantly elevated for the remainder of the study (Supplemental Figure IC). Fasting plasma triglyceride and cholesterol levels were also significantly elevated after 8 and 14 wks on the HF diet respectively (Supplementary Table 1). Other than an unexpected drop in the LF group at the 14 wk time point, fasting plasma glucose levels remained relatively stable and comparable between HF and LF groups over the course of the study (Supplemental Figure ID).

Chronic systemic inflammation is a cardinal feature of obesity and is implicated in the pathogenesis of insulin resistance. Evidence of inflammation in this setting can be found both in tissues (e.g., activation of the intracellular IKK β -NF κ B pathway) and in the form of circulating markers such as cytokines and Serum amyloid A (SAA).¹⁴ As a first step to clarify the time course over which these different humoral responses occur, we obtained serum samples serially over 14 wks from both LF- and HF-fed mice for measurement IL-6, IL-1 β , MCP-1, and SAA. Serum IL-1 β levels remained below detectable limits in both groups at all time points and, neither MCP-1 nor IL-6 levels were significantly elevated by HF feeding during the study (Supplementary Table 2). As a positive control, we demonstrated that mice receiving an acute inflammatory stimulus (injection of lipopolysaccharide at a dose of 50 ng/g IP) showed appropriate elevation of each of these markers. Similarly, SAA levels were not elevated in HF-compared to LF-fed mice until Week 14 (10.6 ± 2.2 vs. 2.3 ± 0.7 $\mu\text{g/ml}$; $p < 0.05$). Together, these findings suggest that circulating markers of inflammation do not increase until late in the course of DIO.

Time course of the effect of high-fat feeding on vascular inflammation and NO production

We next determined the time course over which DIO induces inflammation in vascular tissue and whether this effect is associated with reduced NO content, a measure of endothelial function. Within 1 wk of the onset of HF feeding, induction of phospho-I κ B α (a marker of IKK β activation) was readily detected by Western blot analysis of lysates of thoracic aorta, and this effect persisted throughout the remaining 14 wk study (Figure 1A). Expression of adhesion molecules increases in early atherosclerosis and diabetes,^{15, 16} and these responses constitute additional markers of vascular inflammation and abnormal endothelial function.

Expression levels of vascular cell adhesion molecule-1 (VCAM-1) mRNA were significantly increased after 4 wk of HF-feeding (Figure 1B) and protein levels of intracellular adhesion molecule-1 (ICAM-1) were increased after 2 wk of HF-feeding (Figure 1C). Thus, vascular inflammation and endothelial dysfunction are early manifestations of DIO and occur well prior to any increase of circulating inflammatory markers.

To further assess endothelial function in these thoracic aortic tissue extracts, basal NO levels were measured by ESR.¹² Compared to LF-fed controls, aortic NO levels showed a nonsignificant decrease by week 2 in mice fed the HF diet. This effect of HF feeding achieved statistical significance by 4 weeks and persisted over the remainder of the study (Figure 1D).

Time course of the effect of high-fat feeding on vascular insulin signaling

In human and bovine aortic cell culture models, we have previously shown that activation of IKK β is both necessary and sufficient to explain the impairment of vascular insulin signaling and NO production induced by the saturated FFA, palmitate.⁴ Having demonstrated that IKK β is activated in aortic samples early in the course of DIO, we next sought to determine if this effect is associated with impaired vascular insulin signaling, as assessed by phosphorylation of Akt and eNOS (markers of insulin signal transduction via the IRS-PI3K pathway in vascular tissue) in thoracic aortic lysates 15 min following injection of insulin (0.06 units/g body weight IP) or saline vehicle. Within just 1 wk of HF feeding, the insulin-induced increase of both pAKT and peNOS levels in aortic extracts was significantly attenuated (Figure 2A, B) compared to LF-fed control mice. The early onset of insulin resistance in aortic tissue is therefore linked temporally to the onset of inflammation in this tissue. In addition, the impairment of insulin-induced eNOS activation precedes the decrease of basal (unstimulated) NO content that became significant after 4 wk of HF feeding (Figure 1D).

Effect of high fat-feeding on activation of IKK β in skeletal muscle, liver, and fat

To determine the time course over which DIO is associated with activation of IKK β in liver, muscle, and adipose tissue, lysates of these tissues were analyzed for phospho-I κ B α levels by Western blot analysis. In lysates of both skeletal muscle and liver, phospho-I κ B α became significantly elevated by 8 wk of HF feeding (Figure 3A, B), but not before. TNF- α mRNA levels became significantly elevated by 8 wk of HF feeding in both skeletal muscle (LF: 1 ± 0.06 vs. HF: 2.3 ± 0.32 , $p < 0.05$) and liver (LF: 1 ± 0.12 vs. HF: $1.8 \pm .3$ $p < 0.05$). At the 4-wk time point, however, this effect did not achieve statistical significance in either muscle (LF: 1 ± 0.2 vs. HF: 0.8 ± 0.2 $p = \text{NS}$) or liver (LF: 1 ± 0.12 vs. HF: 1.2 ± 0.31 , $p = \text{NS}$). In adipose tissue, the delay in onset of IKK β activation was even greater and did not achieve statistical significance until 14 wk of high-fat feeding (Figure 3C). Similarly, relative TNF- α mRNA levels did not become significantly elevated in adipose tissue until wk 14 (LF: 1 ± 0.3 vs. HF: 3.25 ± 1 , $p < 0.05$).

Effect of high-fat feeding on liver, skeletal muscle, and adipose tissue insulin signaling

To ascertain whether cellular insulin resistance in liver, muscle, and visceral adipose tissue occurs before, after, or concurrent with the onset of vascular insulin resistance, we measured pAkt content in extracts of these tissues obtained 15 min following IP injection of insulin or vehicle. In skeletal muscle, insulin-mediated Akt phosphorylation tended to be decreased by 4 wk of HF feeding, although this effect did not achieve statistical significance until after 8 wk, and a similar pattern was observed with liver tissue (Figure 4A,B). Like the onset of inflammation, cellular insulin resistance was not detected in adipose tissue until after 14 wk of HF feeding (Figure 4C). Over the course of DIO, therefore, both inflammation and insulin resistance develop in key tissues for glucose homeostasis well after they become evident in the vasculature.

Discussion

To better understand the relationship between obesity and increased risk for cardiovascular disease, we compared the time course over which insulin resistance and inflammation develop in arterial tissue, liver, skeletal muscle, and adipose tissue in a mouse model of DIO. We found that during the first week of HF feeding, insulin resistance and inflammation were clearly evident in aortic tissue, but these responses took far longer to develop in each of the other tissues. Similarly, reduced NO production, a marker of endothelial dysfunction, also occurred relatively early in the course of DIO, and was detected shortly after the onset of vascular insulin resistance. These vascular responses are unlikely to be secondary to circulating inflammatory mediators, as elevated serum levels of SAA and cytokines occurred either weeks later or not at all. Together, these findings suggest that compared to muscle, liver and adipose tissue, vascular elements have an increased susceptibility to the deleterious effects of DIO (Supplementary Figure II).

Our findings extend those of Park, et al., who examined the temporal pattern of changes of insulin sensitivity of both cardiac muscle and tissues involved in glucose metabolism in C57BL/6 mice fed a HF diet (55% from saturated fat)¹⁷. They reported that hyperinsulinemia and impaired insulin-stimulated glucose metabolism in liver, muscle, and adipose tissue occurred after ≥ 3 wk of HF feeding, consistent with the time interval over which fasting plasma insulin levels increased in our study. It is noteworthy that Park, et al. used the glucose clamp technique to measure insulin-stimulated glucose fluxes, whereas our work focused on biochemical assessment of intracellular insulin signal transduction via the IRS-PI3K pathway. A comparison of the two data sets suggests that insulin resistance measured in terms of in vivo tissue glucose handling (evident within 3 wk) slightly precedes the onset of impaired insulin activation of PI3-kinase in insulin target tissues such as skeletal muscle and liver, which in our study became evident between 4-8 wk of HF feeding. A key point, however, is that changes of glucose metabolism in muscle, liver and adipose tissue induced by HF-feeding occur after vascular inflammation and insulin resistance are well established. This conclusion is also supported by Park, et al.'s finding that reduced insulin-stimulated glucose metabolism in heart muscle was evident before detectable changes in systemic glucose handling had occurred (within 1.5 weeks of high fat feeding).¹⁷ These observations lend further support to the hypothesis that vascular tissue is particularly sensitive to the deleterious effects of DIO.

Endothelial-derived NO plays a key role in maintaining normal endothelial function, which includes inhibition of thrombosis and vascular inflammation and maintaining blood pressure and vessel patency. NO also inhibits abnormal growth and vascular inflammation, exerts anti-aggregatory effects on platelets and promotes vasodilation.¹⁸ An important functional consequence of decreased endothelial derived NO is a change in endothelial function favoring inflammation, increased abnormal growth, thrombosis, and vasoconstriction.^{19, 20} Our finding that reduced NO occurs early in the course of DIO raises the possibility that the early onset of vascular dysfunction in this setting could play a key role in the subsequent development of hypertension and atherosclerosis.

The relevance of diet-induced obesity in C57BL6 mice to human obesity warrants comment. Although many mouse models of obesity have been described, common forms of obesity in humans arise from interactions between complex genetic variables and environmental factors including diet composition and physical activity. Thus, mouse models in which obesity arises from a single gene mutation, including leptin-deficient mice (ob/ob), leptin-receptor mutant mice (db/db), and mice with impaired melanocortin receptor function (agouti), are of limited value as models of common human obesity. By comparison, C57BL6 mice maintain normal weight on chow but are genetically predisposed to weight gain on a HF diet, thus resembling human obesity more closely than other mouse models. High fat feeding in C57BL6 mice is

also well established as model of the insulin resistance and glucose intolerance that occurs in human obesity.²¹

The previously documented association between vascular insulin resistance and impaired NO production provides a feasible mechanism linking obesity to decreased NO bioavailability.^{22, 23} Specifically, the generation of NO by endothelial eNOS depends in part on activity of the enzyme, PI3K, which becomes resistant to activation in states of insulin resistance.^{24, 25} These considerations inform the “common-soil hypothesis,” which postulates that vascular disease and diabetes have common antecedents,^{26, 27} and that both have roots in the insulin resistance that develops in states of nutrient overload. Our present results suggest that NO deficiency is an early manifestation of nutrient excess reflecting the heightened susceptibility of endothelium to metabolic stress. The observation that reduced NO bioavailability is an early marker of and risk factor for the development of vascular disease¹⁸ provides additional evidence that this consequence of obesity may be one component of the “common soil” from which vascular disease and insulin resistance develop.

In cell culture models, sensitivity to nutrient excess can vary dramatically between cell types based on differences in metabolic pathways and machinery. At one end of the spectrum, endothelial cells exhibit wide-ranging, deleterious consequences following even brief exposure to excess glucose or FFA, whereas a much greater, more sustained exposure to nutrient excess is necessary to cause toxicity in cell types including pancreatic beta cells and adipocytes.^{28, 29} Although detrimental from the perspective of the whole animal, at the cellular level activation of inflammatory pathways and resultant insulin resistance may serve a protective role by limiting further nutrient uptake. Based on this reasoning, it seems plausible that tissues that evolved to store excess energy (e.g., adipose tissue) or to respond to variation in the level of circulating fuels (e.g., hepatocytes and pancreatic beta cells) would manifest inflammation and insulin resistance well after such responses have occurred in cells that do not actively participate in glucose homeostasis or energy storage, such as are found in vascular tissue. An additional hypothesis supported by our findings is that only after adipose tissue has become insulin-resistant, hence limiting whole body storage of excess fuels, does sustained nutritional excess lead to elevation of circulating markers of systemic inflammation such as SAA and various cytokines.

Many different mechanisms can trigger cellular inflammation in response to nutrient excess, and the nature of these cellular responses can vary between tissues. The differential sensitivity of endothelial cells, hepatocytes, myocytes, and adipocytes to excess nutrients, therefore, likely involves multiple pathways and mechanisms. Furthermore, not all tissues have the same response to inflammatory injury, nor are they equally susceptible to this stress. Thus, the relatively early onset of IKK β -NF- κ B signaling in vascular tissue compared to muscle, liver and fat could reflect differences in the cellular regulation of this enzyme system by accumulation of reactive oxygen species (ROS), long-chain fatty acyl co-A molecules, TLR4 activation, by endoplasmic reticulum stress³⁰ or by mitochondrial dysfunction.^{31, 32} Each of these mechanisms has been forwarded to explain cellular inflammation and insulin resistance during nutrient excess, and additional studies are warranted to determine which of these mechanisms best explains observed temporal differences in the onset of these responses across tissues.

In summary, we report that in a mouse model of DIO induced by HF feeding, vascular inflammation and insulin resistance, along with decreased endothelial NO production, precede the onset of insulin resistance in muscle, liver, and fat, key tissues involved in glucose metabolism. This observation implies a heightened susceptibility of the vasculature to the detrimental effects of nutrient excess relative to tissues involved in glucose homeostasis and fuel storage.

Supplementary Material

Refer to Web version on PubMed Central for supplementary material.

Acknowledgments

A) This study was supported by NIH grants DK073878 (FK), HL30086 (AC), DK52989 and DK68384 (MWS). Body composition studies in mice were performed with support from the Clinical Nutrition Research Unit at the University of Washington supported by NIH grant P30 DK035816. C) Disclosures- none

References

1. Cai D, Yuan M, Frantz DF, Melendez PA, Hansen L, Lee J, Shoelson SE. Local and systemic insulin resistance resulting from hepatic activation of IKK-beta and NF-kappaB. *Nat Med* 2005;11(2):183–190. [PubMed: 15685173]
2. Shoelson SE, Lee J, Goldfine AB. Inflammation and insulin resistance. *J Clin Invest* 2006;116(7):1793–1801. [PubMed: 16823477]
3. Kim F, Tysseling KA, Rice J, Gallis B, Haji L, Giachelli CM, Raines EW, Corson MA, Schwartz MW. Activation of IKKbeta by glucose is necessary and sufficient to impair insulin signaling and nitric oxide production in endothelial cells. *J Mol Cell Cardiol* 2005;39(2):327–334. [PubMed: 15978611]
4. Kim F, Tysseling KA, Rice J, Pham M, Haji L, Gallis BM, Baas AS, Paramsothy P, Giachelli CM, Corson MA, Raines EW. Free fatty acid impairment of nitric oxide production in endothelial cells is mediated by IKKbeta. *Arterioscler Thromb Vasc Biol* 2005;25(5):989–994. [PubMed: 15731493]
5. Jiang ZY, Lin YW, Clemont A, Feener EP, Hein KD, Igarashi M, Yamauchi T, White MF, King GL. Characterization of selective resistance to insulin signaling in the vasculature of obese Zucker (fa/fa) rats. *J Clin Invest* 1999;104(4):447–457. [PubMed: 10449437]
6. Kim F, Pham M, Luttrell I, Bannerman DD, Tupper J, Thaler J, Hawn TR, Raines EW, Schwartz MW. Toll-like receptor-4 mediates vascular inflammation and insulin resistance in diet-induced obesity. *Circ Res* 2007;100(11):1589–1596. [PubMed: 17478729]
7. Senn JJ. Toll-like receptor-2 is essential for the development of palmitate-induced insulin resistance in myotubes. *J Biol Chem* 2006;281(37):26865–26875. [PubMed: 16798732]
8. Vogel RA, Corretti MC, Plotnick GD. Effect of a single high-fat meal on endothelial function in healthy subjects. *Am J Cardiol* 1997;79(3):350–354. [PubMed: 9036757]
9. Keogh JB, Grieger JA, Noakes M, Clifton PM. Flow-mediated dilatation is impaired by a high-saturated fat diet but not by a high-carbohydrate diet. *Arterioscler Thromb Vasc Biol* 2005;25(6):1274–1279. [PubMed: 15774905]
10. Mystkowski P, Shankland E, Schreyer SA, LeBoeuf RC, Schwartz RS, Cummings DE, Kushmerick M, Schwartz MW. Validation of whole-body magnetic resonance spectroscopy as a tool to assess murine body composition. *Int J Obes Relat Metab Disord* 2000;24(6):719–724. [PubMed: 10878678]
11. Kleschyov AL, Mollnau H, Oelze M, Meinertz T, Huang Y, Harrison DG, Munzel T. Spin trapping of vascular nitric oxide using colloid Fe(II)-diethyldithiocarbamate. *Biochem Biophys Res Commun* 2000;275(2):672–677. [PubMed: 10964721]
12. Alp NJ, McAteer MA, Khoo J, Choudhury RP, Channon KM. Increased endothelial tetrahydrobiopterin synthesis by targeted transgenic GTP-cyclohydrolase I overexpression reduces endothelial dysfunction and atherosclerosis in ApoE-knockout mice. *Arterioscler Thromb Vasc Biol* 2004;24(3):445–450. [PubMed: 14707037]
13. Subramanian S, Han CY, Chiba T, McMillen TS, Wang SA, Haw A 3rd, Kirk EA, O'Brien KD, Chait A. Dietary Cholesterol Worsens Adipose Tissue Macrophage Accumulation and Atherosclerosis in Obese LDL Receptor-Deficient Mice. *Arterioscler Thromb Vasc Biol*. 2008
14. O'Brien KD, Chait A. Serum amyloid A: the “other” inflammatory protein. *Curr Atheroscler Rep* 2006;8(1):62–68. [PubMed: 16455016]
15. Price DT, Loscalzo J. Cellular adhesion molecules and atherogenesis. *Am J Med* 1999;107(1):85–97. [PubMed: 10403357]
16. Meigs JB, Hu FB, Rifai N, Manson JE. Biomarkers of endothelial dysfunction and risk of type 2 diabetes mellitus. *Jama* 2004;291(16):1978–1986. [PubMed: 15113816]

17. Park SY, Cho YR, Kim HJ, Higashimori T, Danton C, Lee MK, Dey A, Rothermel B, Kim YB, Kalinowski A, Russell KS, Kim JK. Unraveling the temporal pattern of diet-induced insulin resistance in individual organs and cardiac dysfunction in C57BL/6 mice. *Diabetes* 2005;54(12):3530–3540. [PubMed: 16306372]
18. Harrison DG. Cellular and molecular mechanisms of endothelial cell dysfunction. *J Clin Invest* 1997;100(9):2153–2157. [PubMed: 9410891]
19. Verma S, Anderson TJ. Fundamentals of endothelial function for the clinical cardiologist. *Circulation* 2002;105(5):546–549. [PubMed: 11827916]
20. Liu VW, Huang PL. Cardiovascular roles of nitric oxide: a review of insights from nitric oxide synthase gene disrupted mice. *Cardiovasc Res* 2008;77(1):19–29. [PubMed: 17658499]
21. Lovejoy JC. The influence of dietary fat on insulin resistance. *Curr Diab Rep* 2002;2(5):435–440. [PubMed: 12643169]
22. Kim JA, Montagnani M, Koh KK, Quon MJ. Reciprocal relationships between insulin resistance and endothelial dysfunction: molecular and pathophysiological mechanisms. *Circulation* 2006;113(15):1888–1904. [PubMed: 16618833]
23. Kim JA, Koh KK, Quon MJ. The union of vascular and metabolic actions of insulin in sickness and in health. *Arterioscler Thromb Vasc Biol* 2005;25(5):889–891. [PubMed: 15863720]
24. Zeng G, Quon MJ. Insulin-stimulated production of nitric oxide is inhibited by wortmannin. Direct measurement in vascular endothelial cells. *J Clin Invest* 1996;98(4):894–898. [PubMed: 8770859]
25. Zeng G, Nystrom FH, Ravichandran LV, Cong LN, Kirby M, Mostowski H, Quon MJ. Roles for insulin receptor, PI3-kinase, and Akt in insulin-signaling pathways related to production of nitric oxide in human vascular endothelial cells. *Circulation* 2000;101(13):1539–1545. [PubMed: 10747347]
26. Stern MP. Diabetes and cardiovascular disease. The “common soil” hypothesis. *Diabetes* 1995;44(4):369–374. [PubMed: 7698502]
27. Hu FB, Stampfer MJ. Is type 2 diabetes mellitus a vascular condition? *Arterioscler Thromb Vasc Biol* 2003;23(10):1715–1716. [PubMed: 14555640]
28. Xiao J, Gregersen S, Pedersen SB, Hermansen K. Differential impact of acute and chronic lipotoxicity on gene expression in INS-1 cells. *Metabolism* 2002;51(2):155–162. [PubMed: 11833041]
29. Mordier S, Iynedjian PB. Activation of mammalian target of rapamycin complex 1 and insulin resistance induced by palmitate in hepatocytes. *Biochem Biophys Res Commun* 2007;362(1):206–211. [PubMed: 17698034]
30. Ozcan U, Cao Q, Yilmaz E, Lee AH, Iwakoshi NN, Ozdelen E, Tuncman G, Gorgun C, Glimcher LH, Hotamisligil GS. Endoplasmic reticulum stress links obesity, insulin action, and type 2 diabetes. *Science* 2004;306(5695):457–461. [PubMed: 15486293]
31. Nisoli E, Clementi E, Paolucci C, Cozzi V, Tonello C, Sciorati C, Bracale R, Valerio A, Francolini M, Moncada S, Carruba MO. Mitochondrial biogenesis in mammals: the role of endogenous nitric oxide. *Science* 2003;299(5608):896–899. [PubMed: 12574632]
32. Lowell BB, Shulman GI. Mitochondrial dysfunction and type 2 diabetes. *Science* 2005;307(5708):384–387. [PubMed: 15662004]

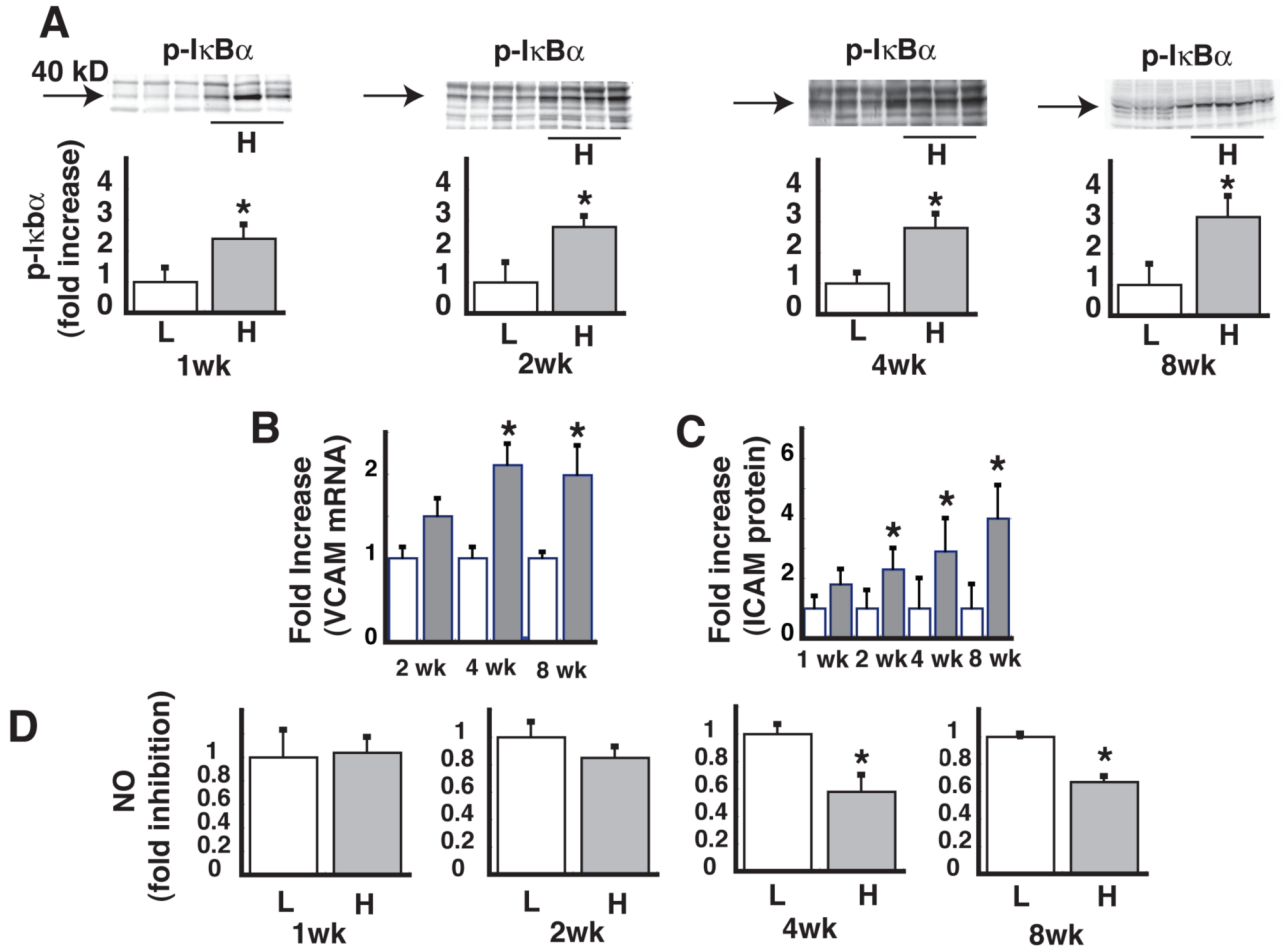


Figure 1. Time course of the effect HF feeding on vascular inflammation and basal NO levels
A. Levels of phospho-IκBα in lysates of thoracic aorta after low fat (L) or high fat (H) feeding, with a representative Western blot for each time point. **B.** Fold increase in VCAM mRNA levels as measured by quantitative PCR. **C.** Fold increase in ICAM protein. **D.** Levels of NO in lysates of thoracic aorta. *P<0.05 vs. LF controls.

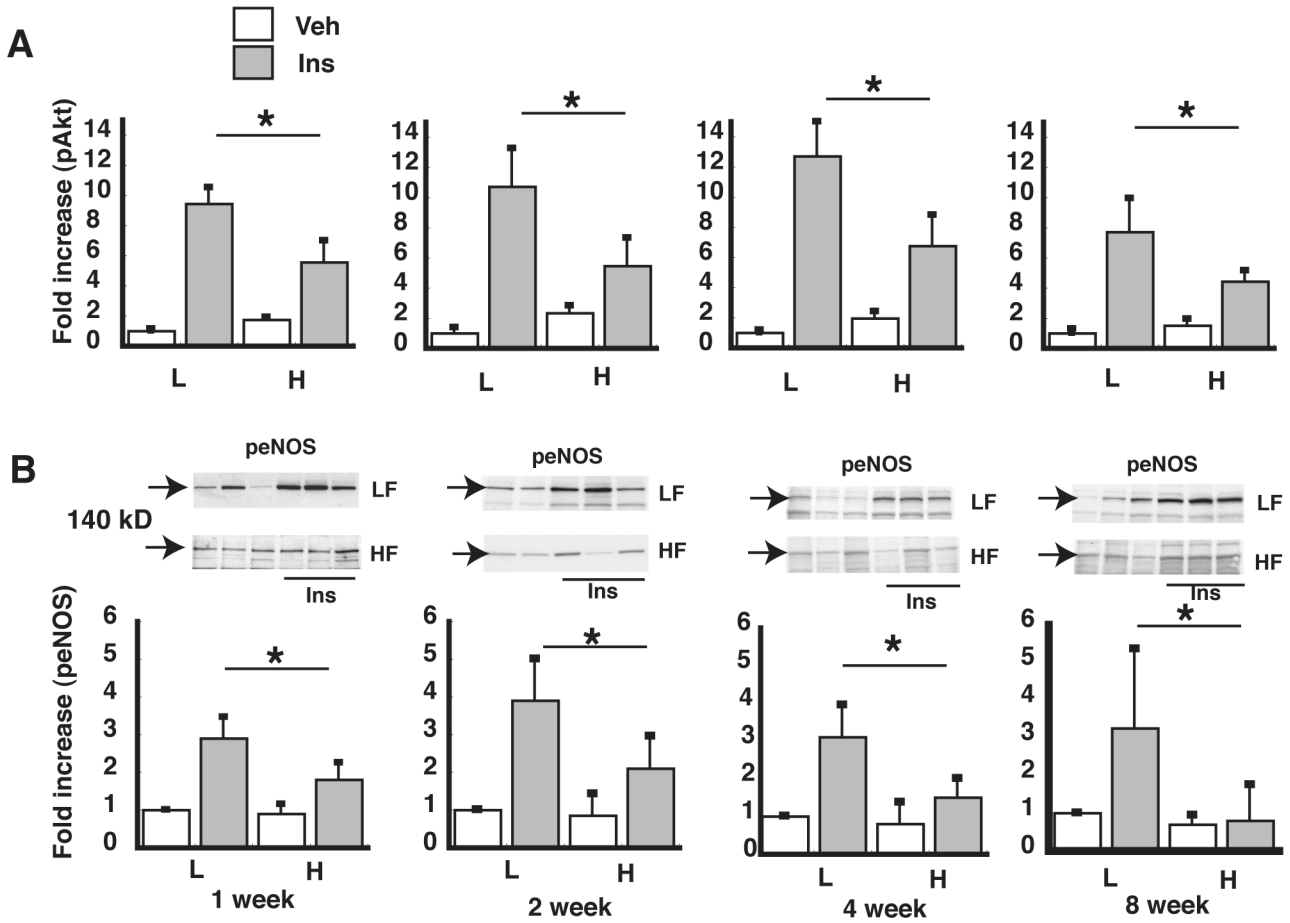


Figure 2. Time course of the effect of HF feeding on vascular insulin signaling

A. pAkt levels in lysates of thoracic aorta as measured by ELISA. For each time point, pAkt levels were normalized to the low fat (L), saline vehicle condition. **B.** peNOS levels in lysates of thoracic aorta as measured by Western blot analysis, quantified using densitometry, and the ratio of peNOS/total eNOS was calculated. *P<0.05 vs. low fat controls (arrow indicates 140 kD molecular weight).

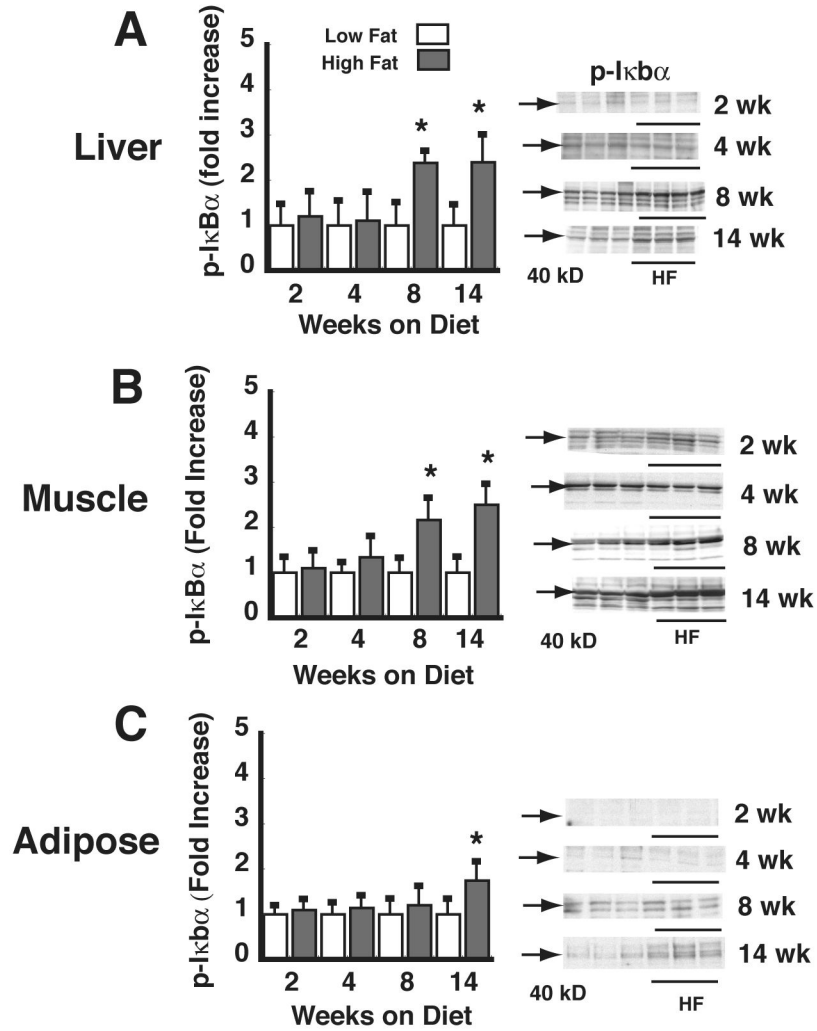


Figure 3. Time course of the effect of HF feeding on liver, muscle, and adipose tissue phospho-IκBα
 Levels of phospho-IκBα were determined in lysates of liver (A), skeletal (quadriceps) muscle (B), and mesenteric adipose tissue (C) by Western blot in mice fed a LF (L) vs. HF (H) diet for periods ranging from 1-14 wk. Data are expressed as fold increase over the LF-fed, vehicle condition. *P<0.05 vs. LF controls. Representative phospho-IκBα Western blots are shown (arrow at 40 kD).

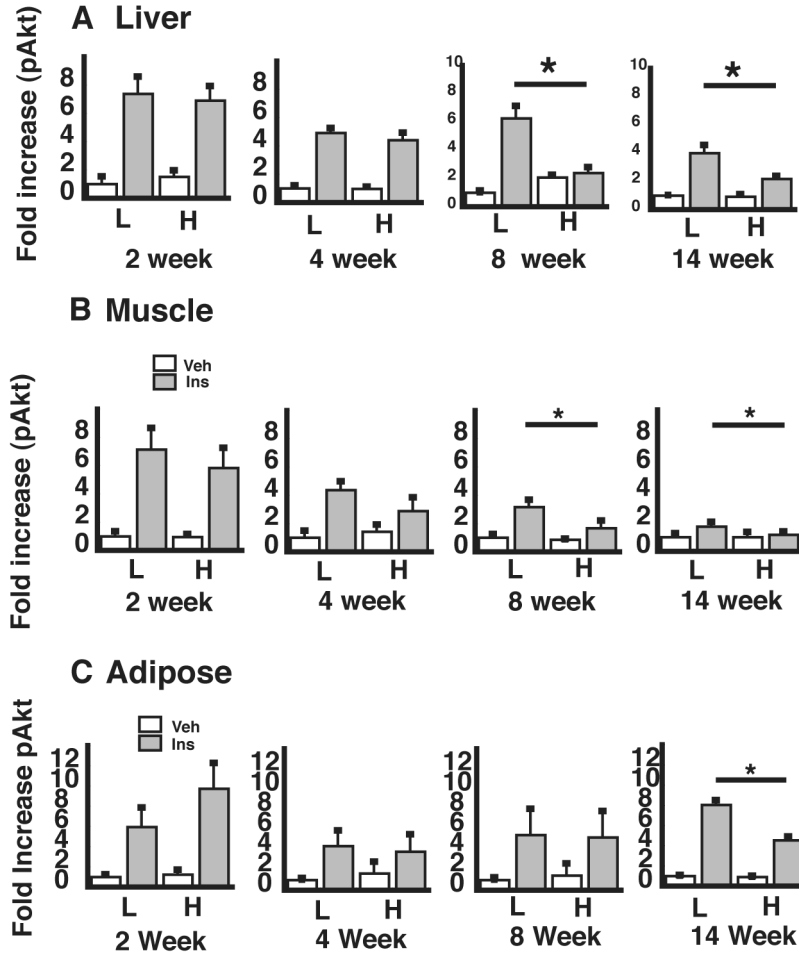


Figure 4. Time course of the effect of HF feeding on insulin signaling in liver, muscle, and adipose tissue
 After consuming a LF (L) or HF (H) diet for periods of 1-14 wk, mice received either saline or insulin. Fifteen minutes later, animals were sacrificed and tissues harvested for analysis of pAkt levels in lysates of liver (A), skeletal (quadriceps) muscle (B), and mesenteric adipose tissue (C). *P<0.05 vs. LF controls.